THE ASTRONOMICAL JOURNAL VOLUME 104, NUMBER 2 AUGUST 1992

RED SUPERGIANTS IN THE SOUTHERN MILKY WAY. I. SEARCH AND CLASSIFICATION TECHNIQUES

D. JACK MACCONNELL[1]
Astronomy Programs, Computer Sciences Corporation, Space Telescope Science Institute, Baltimore, Maryland 21218

ROBERT F. WING[1]
Astronomy Department, Ohio State University, Columbus, Ohio 43210

EDGARDO COSTA[1]
Departamento de Astronomía, Universidad de Chile, Santiago, Chile
Received 27 February 1992; revised 29 April 1992

ABSTRACT

We present a detailed description of a continuing survey for distant, cool supergiants near the galactic plane in the southern hemisphere. Candidate stars are found on near-infrared objective-prism plates, and confirming observations are made with near-infrared narrowband photometry and medium-resolution CCD spectroscopy. The fluxes of 36 southern and equatorial standard stars for the eight-color narrowband system are given. We show how stars are classified in temperature and luminosity type and how the photometry is used to derive distances and reddening. Further papers of the series will present data on the new supergiants found and our conclusions as to distant galactic structure in the southern Milky Way. We expect the survey to result in a several-fold increase in the number of cool supergiants known in the Galaxy.

1. INTRODUCTION

The supergiants of late spectral type are important both in studies of stellar evolution and as indicators of galactic structure. They represent a turning point in the evolution of massive stars at which they attain their largest size and lowest surface temperature. Stars in this range undergo significant mass loss and are often surrounded by extensive circumstellar shells, observable both spectroscopically and through infrared emission from grains. Individually, these stars are interesting as examples of extended atmospheres, the spectra of which can be fully understood only if turbulent motions, spherical geometry, and molecule formation in the outer layers are taken into account.

Because of their high luminosities in the infrared, where interstellar absorption is relatively unimportant, late type galactic supergiants can be detected and recognized at great distances. Hence, if their distances can be determined, their distribution in three dimensions can provide important information about the structure of our Galaxy. In particular, they should be useful as indicators of spiral-arm structure, since in general they are young enough not to have moved very far from their places of birth. Also, if we can learn to detect differences in chemical composition among these supergiants, we can use them to study composition gradients in the Galaxy. Even without measuring any kind of composition parameter in individual stars, we can, in principle, explore abundance gradients in the Galaxy simply by finding and counting the supergiants, since stellar evolution theory (Meylan & Maeder 1983) indicates that the number ratio B/R of blue to red supergiants in any coeval group is a function of the metallicity of the interstellar cloud from which the stars formed. Furthermore, red supergiants are useful as extragalactic distance indicators since they are the brightest stellar objects on red and infrared images of external spirals and appear to have a well-defined upper limit to their luminosity (Humphreys & Davidson 1979).

Despite these attractive features, the late type supergiants, by themselves, have never been used effectively in studies of galactic structure. One problem has been that luminosity classifications—the basis for distance estimates—are hard to assign, especially in the crowded blue spectral region. Another is that the number of supergiants of spectral type M known in the Galaxy prior to this study, for which two-dimensional spectral types confirming their supergiant nature have been published, is only about 200. Most of these have been found in relatively shallow objective-prism surveys and lie within 2 or 3 kpc of the Sun, and the majority are in the northern hemisphere. Our knowledge of distant red supergiants has thus been wholly inadequate for the purpose of tracing spiral arms. Even the statistical use of B/R ratios has not been possible because our knowledge of red supergiants has been far less complete than that of blue ones.

As we will show in this series of papers, a great many more late type supergiants can be identified by means of techniques now available, and their distances can be estimated well enough to encourage applications to problems of galactic structure. The great sensitivity of the infrared CN bands to luminosity and their visibility in all supergiants of types G, K, and M make it possible to deter-

[1]Visiting Astronomer, Cerro Tololo Inter-American Observatory, National Optical Astronomy Observatories.

 0004-6256/92/080821-20$00.90

mine absolute magnitudes and hence distances from observations of low spectral resolution. In particular, White & Wing (1978) have shown how two-dimensional spectral classifications can be obtained for M stars from narrowband photometry on an eight-color near-infrared system, and Warner & Wing (1977) have given examples of distance determinations for heavily reddened stars from the eight-color photometry. Although further calibration work is desirable (and has been undertaken by the authors), it is in principle possible to determine the reddening and distance of any normal (i.e., classifiable) star of late type K or M observed on the eight-color system.

Before the eight-color photometry can be used to identify new late type supergiants, we must have a technique for selecting suitable candidate stars for photometric observation. We would not expect to find many new supergiants among the stars of existing positional or photometric catalogs in which the stars have been selected according to visual or photographic magnitude; indeed, supergiants belonging to distant spiral arms are not likely to have had any previous observation. On the other hand, the low-dispersion near-infrared objective-prism survey of the southern galactic plane conducted by one of us (DJM) is a rich source of supergiant candidates. Details of this survey, which has also been used to discover new carbon stars (MacConnell 1988) and to classify *IRAS* point sources (MacConnell 1989), are given in Sec. 2 below.

Since 1984 we have been conducting follow-up observations, in the form of eight-color narrowband photometry and near-infrared CCD spectroscopy, of supergiant candidates marked in the objective-prism survey; these techniques are discussed in Secs. 3 and 4 below, respectively. The objective of this work is not only to find new supergiants but also to provide two-dimensional classifications and estimates of distance and reddening in order to probe the spiral-arm structure of the Galaxy and the distribution of absorbing material between longitudes 210° and 30°.

Preliminary descriptions of the project have been presented at several IAU symposia and meetings of the AAS (MacConnell & Wing 1984; MacConnell *et al.* 1985, 1986, 1987; Wing *et al.* 1987). Here we discuss in detail the infrared objective-prism search technique used to find supergiant candidates, the photometric and spectroscopic techniques used to classify them in two dimensions, and the procedures used to derive the interstellar reddening and distance. Subsequent papers of this series will present identifications, classifications, and photoelectric data for the supergiants found in various sectors of the southern Milky Way and will consider the luminosity calibration, the distribution of interstellar dust, and our conclusions regarding the spiral-arm structure of the Galaxy as determined from the cool supergiants.

2. THE NEAR-INFRARED OBJECTIVE-PRISM SURVEY

2.1 Characteristics of the Survey Plates

The plates used for the near-infrared survey of the southern Milky Way were taken by D.J.M. with the 61/91 cm Curtis Schmidt camera of the University of Michigan located at Cerro Tololo Inter-American Observatory (CTIO), starting in 1969. The emulsion used was Kodak I-N behind an RG680 filter giving a spectral coverage from 0.68 to 0.88 μm. The 6° and 4° prisms were mounted with their apices rotated 180° to achieve the effective dispersion of a 2° prism; this combination produces spectra 0.5 mm in length with a dispersion of about 3400 Å mm^{-1} at the telluric *A* band. In spite of the small plate scale, 96.6 arcsec mm^{-1}, spectrum overlaps were not a problem at this low dispersion except in the most crowded regions. During the years 1969–1971, unwidened exposures of 5 and 30 min duration were made on separate plates on centers spaced every 4° in galactic longitude on the galactic plane and at $b = \pm 4°$, a total of 138 fields. Starting in 1972, 60 min ammonia-sensitized plates were taken on all of the $b = 0°$ centers and on many of those off the plane. (In recent years, some plates have been taken using other sensitizing methods.) Due to the need to search for guide stars, most plates are shifted from their nominal centers by up to a few tenths of a degree. The approximate limiting I magnitudes are 9, 11, and 13 for the 5 min, 30 min, and sensitized 60 min exposures, respectively. Also taken on the same centers was a set of direct 5 min visual exposures which are used to prepare finding charts to help with the follow-up observations, and to check cases of possible spectrum overlap.

Table 1 gives the nominal plate centers in galactic coordinates, the actual 1950 equatorial coordinates of the center of the deepest plate at each position, and the number of objective-prism plates available in each field. If the number of plates is greater than 2, there is at least one 60 min sensitized plate available on that center. In several fields more than one 60 min exposure was taken in an effort to achieve better spectral resolution (governed by seeing) or a more uniform background. The column "Code" lists a one- or two-letter name, which we use in our preliminary star designations, for each field surveyed to date. The final column gives the number of supergiant candidates marked in each field.

2.2 Selection of Supergiant Candidates

The advantages of the near-infrared spectral region in searches for red supergiants are twofold: (1) these stars have their peak energy output in or near this region, and (2) extinction caused by interstellar dust is half that in the visual region and one-third that in the blue. For these reasons Nassau *et al.* (1954) and Blanco & Münch (1955) used unwidened, near-infrared objective-prism plates to search for M supergiants in the northern and southern Milky Way, respectively. They found that good candidates could be detected as stars showing weak to moderate TiO absorption and a characteristic tapered appearance to their spectra which they attributed to high obscuration. In the present survey, we have relaxed the condition that a star show TiO bands and have marked all stars showing a wedged shape. Thus our selection is based on color and not on any spectroscopic criterion. Unreddened stars of very

TABLE 1. Plate centers for near-infrared survey.

l	b	α (1950)	δ	No.	Code	Candidates
210	-4	06 30.8	+00 45	3	Q	9
210	0	06 42.3	+02 49	3	P	23
210	+4	07 00.1	+04 28	3	R	7
214	-4	06 34.9	-02 32	3	T	86
214	0	06 50.1	-00 44	3	S	31
214	+4	07 07.1	+01 06	4	U	39
218	-4	06 48.9	-06 18	3	AN	32
218	0	06 58.2	-04 16	4	AM	51
218	+4	07 13.3	-02 20	3	AO	27
222	-4	06 52.6	-09 53	3	AP	15
222	0	07 05.2	-07 46	4	V	85
222	+4	07 18.8	-06 02	3	AQ	23
226	-4	07 03.4	-12 27	4	AS	37
226	0	07 12.1	-11 35	4	AR	45
226	+4	07 20.3	-08 36	2	AT	20
230	-4	07 06.0	-16 49	3	AU	65
230	0	07 20.4	-14 55	4	W	56
230	+4	07 37.4	-12 55	4	AV	30
234	-4	07 12.7	-20 29	3	AX	18
234	0	07 29.0	-18 25	3	AW	36
234	+4	07 43.3	-16 38	4	AY	26
238	-4	07 23.6	-24 00	3	AZ	17
238	0	07 38.3	-21 42	4	X	55
238	+4	07 54.3	-19 38	3	BA	26
242	-4	07 31.9	-27 24	4	BC	19
242	0	07 46.9	-25 19	3	BB	40
242	+4	08 02.2	-23 17	4	BD	11
246	-4	07 42.1	-30 20	3	BE	17
246	0	07 57.0	-28 52	3	Y	76
246	+4	08 02.7	-26 46	4	BF	8
250	-4	07 48.8	-34 20	3		
250	0	08 05.8	-32 11	3		
250	+4	08 22.9	-30 00	4		
254	-4	08 00.0	-37 45	5		
254	0	08 18.7	-35 37	3		
254	+4	08 35.6	-33 15	3		
258	-4	08 12.7	-41 05	3		
258	0	08 25.5	-38 38	6		
258	+4	08 44.8	-36 18	7		
262	-4	08 22.0	-44 28	7		
262	0	08 41.5	-41 49	3	BP	50
262	+4	08 56.9	-39 44	3		
266	-4	08 37.4	-47 16	3		
266	0	08 55.8	-45 06	4		
266	+4	09 11.7	-42 29	3		
270	-4	08 54.1	-50 05	5		
270	0	09 12.0	-44 35	3		
270	+4	09 29.4	-45 27	3		
274	-4	09 10.7	-53 59	4		
274	0	09 28.2	-50 35	3		
274	+4	09 41.8	-47 46	5		
278	-4	09 31.0	-56 38	6		
278	0	09 48.6	-53 31	3		
278	+4	10 06.4	-50 25	3		
282	-4	09 54.9	-59 20	3		
282	0	10 09.8	-55 42	3		
282	+4	10 26.3	-52 18	3		
286	-4	10 21.6	-61 20	4		
286	0	10 32.1	-58 10	5		
286	+4	10 49.4	-54 31	4		
290	-4	10 50.6	-63 33	4	C	12
290	0	10 57.1	-60 08	6	A	77
290	+4	11 16.2	-56 05	4	D	16
294	-4	11 25.5	-64 53	3	G	37
294	0	11 31.0	-61 36	3	E	44
294	+4	11 42.8	-57 31	4	F	26
298	-4	12 01.7	-65 42	4	I	32
298	0	12 02.5	-62 16	3	H	50
298	+4	12 12.8	-58 15	4	J	22
302	-4	12 42.2	-66 32	3	Z	23
302	0	12 38.2	-62 48	5	M	73
302	+4	12 42.7	-58 27	5	N	11
306	-4	13 21.4	-66 22	4	AC	40
306	0	13 09.9	-62 28	3	AA	92
306	+4	13 10.3	-58 22	3	AB	31
310	-4	13 58.7	-65 35	3	AE	20
310	0	13 42.1	-61 44	3	AD	63
310	+4	13 40.0	-57 42	6	AF	29
314	-4	14 34.4	-64 21	3	AH	16
314	0	14 13.9	-60 28	3	AG	39
314	+4	14 08.6	-57 00	3	AI	21
318	-4	15 07.1	-62 35	3	AK	73
318	0	14 46.7	-59 31	3	AJ	88
318	+4	14 35.1	-55 40	3	AL	67
322	-4	15 36.1	-60 24	3	BH	52
322	0	15 11.3	-57 28	3	BG	65
322	+4	15 02.2	-53 11	3	BI	54
326	-4	15 59.0	-57 42	4	BK	75
326	0	15 38.0	-54 52	3	BJ	77
326	+4	15 27.7	-51 43	3	BL	44
330	-4	16 20.5	-54 56	3	BN	80
330	0	15 56.9	-52 04	3	BM	44
330	+4	15 43.1	-49 18	4	BO	50
334	-4	16 41.3	-52 31	4		
334	0	16 20.8	-49 34	3		
334	+4	16 06.8	-46 32	3		
338	-4	16 50.0	-49 27	4		
338	0	16 35.5	-46 13	4		
338	+4	16 29.3	-43 20	4		
342	-4	17 08.4	-45 39	3		
342	0	16 49.5	-43 42	3		
342	+4	16 36.6	-40 44	3		
346	-4	17 20.7	-42 53	4		
346	0	17 04.7	-40 24	4		
346	+4	16 49.1	-37 53	4		
350	-4	17 34.4	-39 40	4		
350	0	17 14.4	-36 52	5		
350	+4	17 00.8	-34 37	4		
354	-4	17 46.8	-36 03	4		
354	0	17 24.2	-34 12	6		
354	+4	17 11.8	-31 41	5		
358	-4	17 52.5	-32 01	3		
358	0	17 37.5	-30 24	5		
358	+4	17 22.7	-27 57	4		
002	-4	18 00.6	-29 27	3		
002	0	17 49.6	-26 45	3		
002	+4	17 33.1	-24 35	3		
006	-4	18 11.1	-25 27	3		
006	0	17 56.8	-23 40	4		
006	+4	17 40.3	-21 13	3		
010	-4	18 21.4	-21 30	3		
010	0	18 00.5	-20 18	3		
010	+4	17 50.1	-17 58	2		
014	-4	18 26.1	-19 00	2		
014	0	18 11.8	-16 48	3		
014	+4	17 52.3	-14 14	3		
018	-4	18 33.3	-15 12	2		
018	0	18 21.7	-13 15	4		
018	+4	18 06.4	-11 37	2		
022	-4	18 42.5	-11 30	2		
022	0	18 26.9	-09 37	4		
022	+4	18 14.5	-08 15	2		
026	-4	18 47.8	-08 12	3		
026	0	18 36.0	-05 49	3		
026	+4	18 20.1	-04 28	2		
030	-4	18 56.4	-04 23	3		
030	0	18 42.7	-02 46	3		
030	+4	18 28.8	-01 18	2		

late type may be equally red but have a different appearance due to the presence of strong TiO and VO bands, and such stars are not marked in our survey. Wedge-shaped spectra can also be presented by heavily reddened early type stars, and indeed several new supergiants of types A and F have been found in this survey (see, for example, MacConnell *et al.* 1987), but experience has shown that relatively few such stars will appear on infrared plates.

The present study was undertaken to find fainter and more distant cool supergiants by using both lower dispersion and longer exposures than were used in previous surveys. Our deep plates have six times the exposure for those used in the Blanco–Münch survey, while our dispersion is a factor of 2 lower, and our ammonia sensitization adds approximately another factor of two. The net effect of these differences is to extend the limiting magnitude by about 3.5 mag. Whereas Blanco and Münch were able to find supergiants in the neighboring Sagittarius and Carina Arms, we can expect to detect similar stars at distances up to five times as great.

The spectrum plates are scanned visually by D.J.M. using a binocular microscope at a magnification of 12 diameters. Each plate is examined independently of others on that center searching for stars having a tapered form (with the point at the short-wavelength end). Stars with strong TiO bands are expected to be normal M giants and are not marked. Stars noted as of interest on separate plates of the same field are reexamined on the best deep plate, and a single list of candidates is compiled for that field. The final column of Table 1 gives the number of stars marked as cool supergiant candidates in the fields surveyed to date. A total of 2600 candidates have been marked thus far in 46% of the fields.

We do not mean to imply that more than 5600 late type supergiants can be identified on our plates. For one thing, the number of candidates should be reduced by about 16% to allow for plate overlap. More important, because of the very small scale of our survey spectra, we cannot expect a very large fraction of the candidates to be *bona fide* supergiants. Statistics reported by Wing *et al.* (1987), based on the follow-up observations then available, indicated that about 30% of the candidates tested were, in fact, more luminous than luminosity class II. We have subsequently found that there are some regions of the galactic plane that are relatively devoid of supergiants and where the percentage of candidates confirmed as supergiants is lower, perhaps 20%. At this point our best estimate is that approximately 25% of the candidates marked on the survey plates will be confirmed as supergiants.

If this success rate seems low, we should clarify the nature of the candidate selection process. The criterion of tapered shape is necessarily subjective and depends critically on the seeing, focus, and plate background. Only a minority of the candidates show the tapered shape strongly and clearly; most of these are true supergiants, although a few turn out to be stars of type S as discussed in Sec. 4 below. The majority of the candidates have less distinct shapes, and many are borderline cases that could equally well be marked as candidates or not. In a sample of 14 overlapping 60 min plates, only 26% of the candidates in the regions of overlap had been marked independently on both plates. Unfortunately, supergiants which suffer relatively little reddening cannot be distinguished on the survey plates from ordinary early M giants of moderate reddening; since our aim has been to find as many new supergiants as possible, including those which are not heavily reddened, we must include a large number of ordinary giants on our list of candidates. A success rate of 25% would hardly be satisfactory if we were merely publishing the list of candidates and leaving the follow-up work to others. However, we have efficient techniques at our disposal for determining luminosity classes of the candidate stars, and it is our intention to publish two-dimensional classifications for all stars identified in this project.

2.3 Equatorial Coordinates and Charts

Part of the task of surveying a field is determining the coordinates of each star marked as a supergiant candidate. These measurements have been made, by D.J.M., on a variety of instruments over a span of two decades. Most of the earlier measurements were made at Case Western Reserve University, where equatorial coordinates of candidates were measured on the deepest spectrum plate of each field relative to a grid of eight SAO reference stars well distributed over the plate. More recently, positional measures have been made using the *HST* Guide Star Astrometric Support Program (GASP), developed at the Space Telescope Science Institute from plate scans used for the *HST Guide Star Catalogue* (Lasker *et al.* 1990). The positional errors are at most a few arcsec in each coordinate.

We have been using a Polaroid Land camera to make enlargements from the direct visual plates for our own use during the follow-up observations. We expect to use GASP to produce finding charts for publication.

3. CLASSIFICATION PHOTOMETRY

The red stars marked as supergiant candidates in our objective-prism survey would be of little value in galactic-structure applications if we did not have a way of knowing which ones are true supergiants and a consistent method of estimating their distances. Confirmation of supergiants requires classification on a system sensitive to luminosity differences among late type stars, e.g., MK classification, or the photometric measurement of a luminosity-sensitive spectral feature. Distance determination requires, in addition, the measurement of an apparent magnitude, a method for correcting this magnitude for interstellar absorption, and the calibration of the spectroscopically derived luminosity class (or the luminosity criterion itself) in terms of absolute magnitude.

We have chosen the eight-color near-infrared system of narrowband photometry introduced by Wing (1971) as our primary technique for follow-up work because observations on this system, together with its associated calibrations, provide all the information needed to determine the distances of red supergiants. In particular, the eight-color photometry provides the following:

(1) An apparent magnitude, $I(104)$, measured at 10 400 Å in a region nearly always free of significant atomic or molecular blanketing.

(2) A color index indicating the slope of the near-infrared continuum.

TABLE 2. Properties of interference filters.

Filter	λ_c (Å)	$\Delta\lambda$ (Å)	Feature measured
1	7120	60	TiO γ(0,0) band; also CN
2	7540	50	Continuum; weak CN
3	7810	40	TiO γ(2,3) band
4	8120	50	CN (3,1) band
5	10395	50	Continuum; I(104)
6	10540	60	Continuum; VO for Sp. ≧ M6
7	10810	60	Continuum
8	10975	70	CN (0,0) band

(3) A measurement of one of the strongest TiO bands, which can be detected in stars as early as type K3.5.

(4) An index of the strength of the Red System of CN, based in part on the strong, uncontaminated (0,0) band at 11 000 Å.

The indices of TiO and CN, which respond to temperature and luminosity, respectively, are used for two-dimensional classification. The interstellar reddening can then be found by comparing the observed color to the intrinsic color corresponding to the observed spectral type, and the interstellar absorption at 10 400 Å can be inferred from the reddening by assuming a normal interstellar reddening law. Finally, the distance is found by comparing the corrected apparent $I(104)$ magnitude to the absolute magnitude indicated by a calibration of the luminosity class or CN index. These procedures and calibrations are discussed in detail in the following sections.

3.1 Filter and Detector Characteristics

The properties of the interference filters defining the eight-color system are given in Table 2. Their central wavelengths λ_c range from 0.7 to 1.1 μm in the near infrared; their widths $\Delta\lambda$ (these are full widths measured at half the peak transmission) average about 55 Å, although filters 1 and 8, which measure strong bands of TiO and CN and are therefore often strongly depressed, were made somewhat wider than the average.

The filter sets in current use were manufactured in 1978 by MicroCoatings, Inc., and have retained their original transmission properties well. The values given for λ_c and $\Delta\lambda$ in Table 2 are the nominal values used in placing the order; the measured values differ slightly from set to set but are all well within the specified tolerances of ± 10 Å in both quantities. Nearly all the observations for this program to date have been obtained with the filter set acquired by CTIO, although a set belonging to the Ohio State University has also been used. Another essentially identical set is available at KPNO. The reductions of standard-star observations show no evidence of systematic differences between the filter sets.

The filters were chosen to measure the strongest near-infrared bands of TiO, CN, and VO as indicated in the last column of Table 2. The VO molecule appears only in stars of type M6 and later and is rarely encountered among the stars of this program; the bands of TiO and CN, on the other hand, are seen in all late K and M giants and supergiants, and they provide the basis for their two-dimensional classification. The filter widths were chosen to maximize the system's sensitivity to these absorption features and also its ability to avoid the bands of these molecules in order to measure the continuum. By including filters that are nearly free of blanketing in two widely separated wavelength regions, the system offers a means of measuring useful color temperatures as well as establishing a continuum with respect to which the molecular absorptions can be measured.

The filters are sufficiently narrow that the sensitivity function of the detector plays no role in defining the system, other than to set the zero points used in transforming from the instrumental to the standard system. Thus any detector that responds throughout this wavelength region can be used, and no color terms are involved in the reductions. Unfortunately there are few photometric detectors available for work in the 1 μm region. The eight-color system was originally set up (Wing 1971) using photomultipliers with S-1 photocathodes, but they have such low quantum efficiency (maximum $\sim 0.1\%$) that a large telescope would be needed to reach typical stars of the present program. It is the availability of a Varian LSE cell, Model 159A (InGaAsP cathode), at CTIO that has made this project feasible. Our comparisons show that the Varian cell at CTIO is 40 times more sensitive than CTIO's best S-1 cell over the wavelength range covered by filters 1–6, although the difference is not so large at the longest wavelengths, dropping to only a factor of 3 at filter 8. Nearly all the photometry for this project has been obtained with the Yale 1.0 m telescope at CTIO, with the Varian cell and ASCAP single-channel photometer.

3.2 Standard Stars and Absolute Calibration

The eight-color system may be considered to be defined by the magnitudes of 90 bright standard stars of all types published by Wing (1979). These stars are well distributed about the sky in both hemispheres, and their magnitudes have been carefully tied together through a decade of observation with S-1 cells. Unfortunately, most of these stars are too bright to observe with a 1.0 m telescope and the much more sensitive Varian cell, which has a strict upper limit of 2×10^5 counts s^{-1} to its anode current. Therefore a set of fainter standards was added to the system starting in 1978 when Varian cells became available at both KPNO and CTIO.

The 48 new standards are all of spectral types F, G, and K and of luminosity classes III, IV, and V, since such stars are less likely to be variable than hotter, cooler, or more luminous stars, and since there are no color terms that need to be evaluated for the reductions. Their visual magnitudes are around 6.0–6.5, and their near-infrared magnitudes are bright enough to be observed comfortably in all 8 filters at a 1.0 m telescope without being too bright

TABLE 3. Fluxes of faint standard stars.

BS	Name	Spectral Type	V	Adopted Magnitudes 7120	7540	7810	8120	10395	10540	10810	10975
	A) Faint Equatorial Standards										
107		F6 V	6.04	4.485	4.595	4.677	4.788	5.381	5.405	5.487	5.572
448		G2 IV	5.76	4.063	4.168	4.224	4.318	4.874	4.893	4.991	5.051
616		K0	6.28	4.449	4.487	4.519	4.658	5.020	5.043	5.127	5.259
988	14 Eri	F1 V	6.14	4.594	4.705	4.795	4.896	5.528	5.565	5.642	5.716
1446		G8 III	6.01	4.043	4.054	4.072	4.180	4.515	4.507	4.577	4.684
1970		K4 III	6.31	4.047	3.871	3.898	3.940	4.111	4.117	4.162	4.249
2313		F8 V	5.87	4.235	4.325	4.404	4.484	5.060	5.089	5.171	5.255
3033		G0	6.53	4.727	4.799	4.838	4.922	5.410	5.431	5.511	5.579
3424		K1 III	6.45	4.501	4.530	4.531	4.665	4.990	4.996	5.080	5.194
3649		A9 IV	6.35	4.875	4.991	5.083	5.193	5.845	5.881	6.000	6.098
4253		G8 III	5.45	3.567	3.609	3.633	3.755	4.146	4.157	4.227	4.331
4478		K1 III	6.17	4.237	4.266	4.271	4.410	4.733	4.736	4.818	4.949
4657		F5 V	6.11	4.518	4.606	4.677	4.762	5.363	5.391	5.470	5.549
5183		G0-1 IV-V	6.33	4.640	4.741	4.792	4.877	5.466	5.486	5.579	5.642
5536		K3 III	6.18	3.981	3.921	3.912	4.036	4.195	4.187	4.251	4.347
5721	8 Ser	F0 V	6.12	4.706	4.845	4.944	5.065	5.723	5.762	5.860	5.975
6124		G8 III	6.07	4.195	4.246	4.279	4.390	4.801	4.810	4.875	4.960
6390		K0 III	6.33	4.353	4.380	4.408	4.510	4.850	4.860	4.915	5.000
6844		F2 V	6.63	5.153	5.290	5.378	5.500	6.143	6.181	6.260	6.382
7321	24 Aql	K0 IIIa	6.41	4.445	4.470	4.490	4.623	4.937	4.963	5.027	5.134
7809		gK1	6.11	4.031	4.036	4.043	4.179	4.443	4.461	4.539	4.605
8205		F5 V	6.13	4.529	4.650	4.722	4.835	5.471	5.484	5.606	5.668
8530		G6 III Ba	5.93	4.040	4.065	4.088	4.240	4.617	4.623	4.705	4.848
8934	13 Psc	K1 III	6.38	4.356	4.365	4.367	4.488	4.744	4.761	4.829	4.934
	B) Faint Southern Standards										
358		F7 IV	6.52	4.940	5.051	5.128	5.226	5.840	5.873	5.963	6.038
1031		K0	6.50	4.362	4.307	4.301	4.445	4.636	4.642	4.700	4.818
1766		F2 IV-V	6.34	4.869	5.001	5.095	5.200	5.831	5.874	5.960	6.068
2685		gG0	6.11	4.336	4.424	4.482	4.562	5.092	5.113	5.204	5.272
3729		K1 III	6.54	4.559	4.566	4.571	4.721	5.016	5.024	5.090	5.209
4373		F4 V	6.45	4.875	4.982	5.061	5.156	5.770	5.800	5.883	5.970
4999		K1 III	6.19	4.275	4.314	4.336	4.458	4.844	4.856	4.933	5.020
5689		G6 III-IV	6.20	4.252	4.295	4.325	4.415	4.800	4.814	4.876	4.947
6454		F7 V	6.47	4.777	4.877	4.950	5.042	5.631	5.657	5.737	5.811
7330		G5 V	6.48	4.754	4.843	4.904	4.990	5.547	5.577	5.670	5.730
8124		K0	6.12	3.918	3.870	3.874	3.975	4.174	4.180	4.250	4.356
8914		K2	6.32	4.297	4.290	4.300	4.439	4.702	4.711	4.780	4.886
	C) Primary Standard (Vega)										
7001	α Lyr	A0 Va	0.03	-1.145	-0.950	-0.830	-0.695	0.000	0.050	0.155	0.320

in any filter at telescopes up to 2.0 m in aperture. Initially, 24 equatorial standards—one in each hour of right ascension—were chosen and tied to the 90 original standards through observations from both KPNO and CTIO. By themselves, the equatorial standards have the drawback that they never pass close to the zenith at observatories at temperate latitudes and are therefore less than ideal for extinction measurements. Consequently 24 additional faint standards, 12 with declinations between +30° and +40° and another 12 with declinations between −30° and −40°, were selected and tied to the equatorial standards.

In Table 3 we present the adopted magnitudes of the new equatorial and southern standards. They form a carefully iterated set after repeated reductions of observations obtained over a period of more than 10 yr. Most of these stars have been observed more than 100 times and we believe that their magnitudes are known as accurately as those of the standards of any photometric system. The

spectral types and V magnitudes listed in Table 3 are from the *Bright Star Catalogue* (Hoffleit & Jaschek 1982). At the end of the table the corresponding magnitudes of Vega (α Lyr), one of the 90 original standards, are given as a way of specifying the system calibration.

The magnitudes of standard stars, and hence also of program stars reduced with respect to them, are expressed on a system of absolute fluxes per unit wavelength interval. The use of an absolute scale allows the observed energy distributions to be compared directly to flux distributions of blackbodies or model atmospheres, so that temperatures can be obtained from the colors. In addition, the set of eight magnitudes for any star, when plotted against wavelength, can be treated as a spectrum.

Since the magnitudes of standards have been tied together by the observations, we need only assume an absolute energy distribution for one star in order to place the whole set on an absolute scale. We have assumed that α Lyr (Vega) can be represented by the model-atmosphere energy distribution chosen by Schild *et al.* (1971) to fit the available absolute flux measurements of that star. More recent calibration work (e.g., Hayes *et al.* 1975) and comparisons with models (e.g., Kurucz 1979) have led to the choice of somewhat different models for α Lyr, but the slope of the near-infrared continuum has been left unchanged. The assumed fluxes for α Lyr given in Table 3 have been derived from Table 5 of Schild *et al.* (1971), after conversion from frequency to wavelength units and renormalization. The zero point of the whole system of fluxes has been set by adopting a magnitude of 0.00 for α Lyr in filter 5 at 10 400 Å; this magnitude, called $I(104)$, is the one normally used when stellar apparent magnitudes are discussed because it remains a good continuum point in even the coolest M stars (Wing 1967a).

3.3 Photometric Reductions

The photometric data for this project are reduced relative to the standard stars listed in Table 3. Extinction and transformation coefficients are measured on every night of observation, normally from between 20 and 25 observations of standard stars. An effort is made to distribute the observations of standards fairly uniformly in time and randomly in airmass. No distinction is made between extinction stars and transformation standards; rather, all observations of standards obtained during a night are used together in a single least-squares solution for the extinction and transformation coefficients at each wavelength. The transformation coefficients here are simply the zero points needed to convert from the instrumental system to the standard system; the filters are sufficiently narrow that no color terms are needed in the transformations.

Extinction coefficients appropriate for Cerro Tololo in the filters of the eight-color system are given in Table 4. The mean values are not actually used in the reductions but are listed for illustrative purposes. We do impose upper and lower limits to the extinction coefficients that can be used in the reductions to guard against using the occasional unrealistic computed value, and these limits are also

TABLE 4. Extinction coefficients for Cerro Tololo.

λ_c(Å)	Coefficient (mag/air mass)		
	Mean	Min.	Max.
7120	0.070	0.040	0.090
7540	.050	.025	.080
7810	.045	.025	.080
8120	.065	.030	.090
10395	.030	.015	.055
10540	.035	.020	.055
10810	.035	.020	.060
10975	.050	.030	.080

tabulated in Table 4. Since Rayleigh scattering is almost negligible at these wavelengths and the filters were chosen to avoid the important telluric bands of H_2O and O_2, the coefficients are quite small and the uncertainties in their values are seldom a significant source of photometric error. On nights of high absolute humidity we do see an increase in the measured coefficients in filters 1, 4, and 8 which contain weak lines of H_2O, but we have no evidence that the true coefficients on clear nights at Cerro Tololo ever fall outside the maximum and minimum values tabulated.

The residuals of standard stars indicate that the errors in the magnitudes obtained from single observations, on most nights, are in the range 0.007–0.010 mag. The eight residuals for a given star tend to be strongly correlated, so that the errors in differential quantities (colors and band-strength indices) are smaller, in the range 0.005–0.007 mag. The same accuracy is normally achieved for program stars as for standards in filters 1–6, where the Varian cell has good sensitivity, but the accuracy for the fainter program stars in filters 7 and 8 may be impaired by the rapidly decreasing cell sensitivity and the correspondingly greater importance of photon statistics. We normally collect at least 20 000 counts above sky in each filter to ensure that the final accuracy is not photon-noise limited, but for faint stars this total is not always reached in filter 8. Because of the importance of the (0,0) band of CN as an indicator of absolute magnitude, it is worthwhile spending more time measuring filters 7 and 8 than the other filters, and it is not unusual to devote more than half the total integration time on a faint star to measuring this pair of filters. Even so, the estimated errors in the magnitudes are largest in these filters, usually in the range 0.010–0.015 mag for program stars depending on their brightness.

There is another problem that had to be recognized and dealt with before the accuracy quoted above could be achieved: the sensitivity of CTIO's Varian cell is not stable in the long-wavelength tail of its response function (longward of $\sim$10 600 Å). Initially, the reductions of standard stars showed large residuals in filters 7 and 8—much larger than expected from photon statistics—even on nights which reduced very well in filters 1–5. Eventually the problem was traced to the temperature sensitivity of the cell's

response in its long-wavelength tail. Because of the small capacity of the Varian cell's dry-ice cold box, it is not possible to maintain a constant temperature for more than about 4 h, and when the box is opened to add dry ice, the cathode temperature is raised further. Furthermore, after refilling, the cathode temperature drops slowly for 1–2 hr before stabilizing, during which time data collection must proceed. Changes in cathode temperature have no perceptible effect on cell sensitivity in the wavelength range of filters 1–5 (7000–10 500 Å) but are positively correlated with sensitivity changes at longer wavelengths.

Installation of a digital thermometer with remote readout helped us to understand these temperature changes and to develop observing procedures that normally limit the sensitivity changes to no more than ±5% in filter 8. However, because of hysteresis between the recorded temperature changes and the sensitivity changes seen in the residuals of standard stars (probably due to not measuring the temperature exactly at the photocathode), we have not been able to derive satisfactory sensitivity corrections directly from the temperature readings. Rather, our correction procedure relies upon the standard-star residuals and is successful only because of the large number of standard-star observations normally obtained.

A night of observation is first reduced by the all-sky method described above, and the residuals for standard stars in filters 6–8 are plotted against the time of observation. Smooth curves are drawn through the points to represent our best estimate of the cell's actual sensitivity variation with time; the curves for filters 6–8 are drawn with the same phasing but different amplitudes, roughly in the proportion 1:4:5, respectively, and often the corrections for filter 6 are so small that they can be neglected. These curves are then read back into the computer so that corrections to the fluxes of both program and standard stars can be computed as a function of time. Of course, the residuals shown by standard stars following these corrections are artificially low; the corrections are applied not to improve the appearance of the standard-star reductions but to obtain the best possible reductions for the program stars.

Our correction procedure depends upon the availability of accurately known magnitudes for the standard stars. Before these corrections were introduced, the magnitudes of standard stars were poorly known in filters 7 and 8 because of the sensitivity changes affecting previous observations, and consequently it was difficult to ascertain the behavior of the cell. Determination of both the standard magnitudes and the nightly sensitivity corrections required a long series of iterations involving data from several observing runs spread over several years.

It should be stressed that time-dependent corrections are never needed in filters 1–5, and that they seldom exceed 1% in filter 6. Also, the Varian cell at KPNO has not shown sensitivity changes of this sort, although we have often used it to observe at the same set of wavelengths. Even in the long-wavelength CTIO data, the errors in the corrected photometry are serious only in the older data obtained before the problem was recognized. Whether or not the older data can be successfully reduced is a question of the frequency and timing of the observations of standards. A few observations have been thrown out because they were made at times when the sensitivity curves were not adequately defined. On most nights, however, the sensitivity curves have small enough amplitudes and are well enough defined that uncertainties in the corrections are no larger than other sources of error such as counting statistics or changes in dark current, either of which can be significant in filters 7 and 8.

The reductions to date have been carried out primarily at the Ohio State University using programs written for OSU's IBM 3081 mainframe computer. The software package has also been restructured and transported to CTIO where it can be used on the Observatory's SUN computers.

3.4 Color Temperatures and Band-Strength Indices

The reduced eight-color photometry for representative stars of several spectral types is shown in Fig. 1. The stars include, on the left, a solar-type dwarf, a K supergiant, and a carbon star, and on the right two M stars, one of which is heavily reddened. The latter star, which has the provisional designation A-30 and is located at $\alpha = 11{:}00{:}23.4$, $\delta = -61{:}22{:}01$ (1950), is one of the M supergiants found in this program. The shapes of the spectra are governed by four variables: the temperature and interstellar reddening, which together determine the slope of the continuum, the TiO strength, which depends primarily upon the star's intrinsic temperature, and the CN strength, which in oxygen-rich stars depends primarily upon the luminosity. The main features of TiO and CN which appear in the eight-color spectra are marked in Fig. 1 and identified in Table 2.

To judge which filters are depressed by absorption features and to obtain quantitative measures of band strength, it is helpful to know the level of the stellar continuum. Since the filters fall into two wavelength groups (filters 1–4 and 5–8) separated by ~3000 Å, a good approximation to the continuum is established by the photometry whenever there is at least one good continuum point in each group, and the filters were chosen with this point in mind. We therefore proceed by finding the blackbody curve that passes through the point of least blanketing in each group of four filters. As Wing (1967b) has shown, for any dataset there exists a unique solution, which can be found by a simple iterative routine, for the blackbody curve that passes through one point in each group and above all other points. This curve, of course, does not correspond precisely to the true stellar continuum; no filters are completely free of absorption lines, and in any case the true continuum does not have the shape of a blackbody curve, being modified by the wavelength dependence of H^- opacity and other continuous absorbers. Nevertheless, the blackbody curve found in this manner is a reasonable approximation to the true continuum in most types of stars (exceptions being the M stars later than M6, and some S stars), and it provides a useful starting point in the analysis of the photometric data.

The temperature corresponding to the fitted blackbody

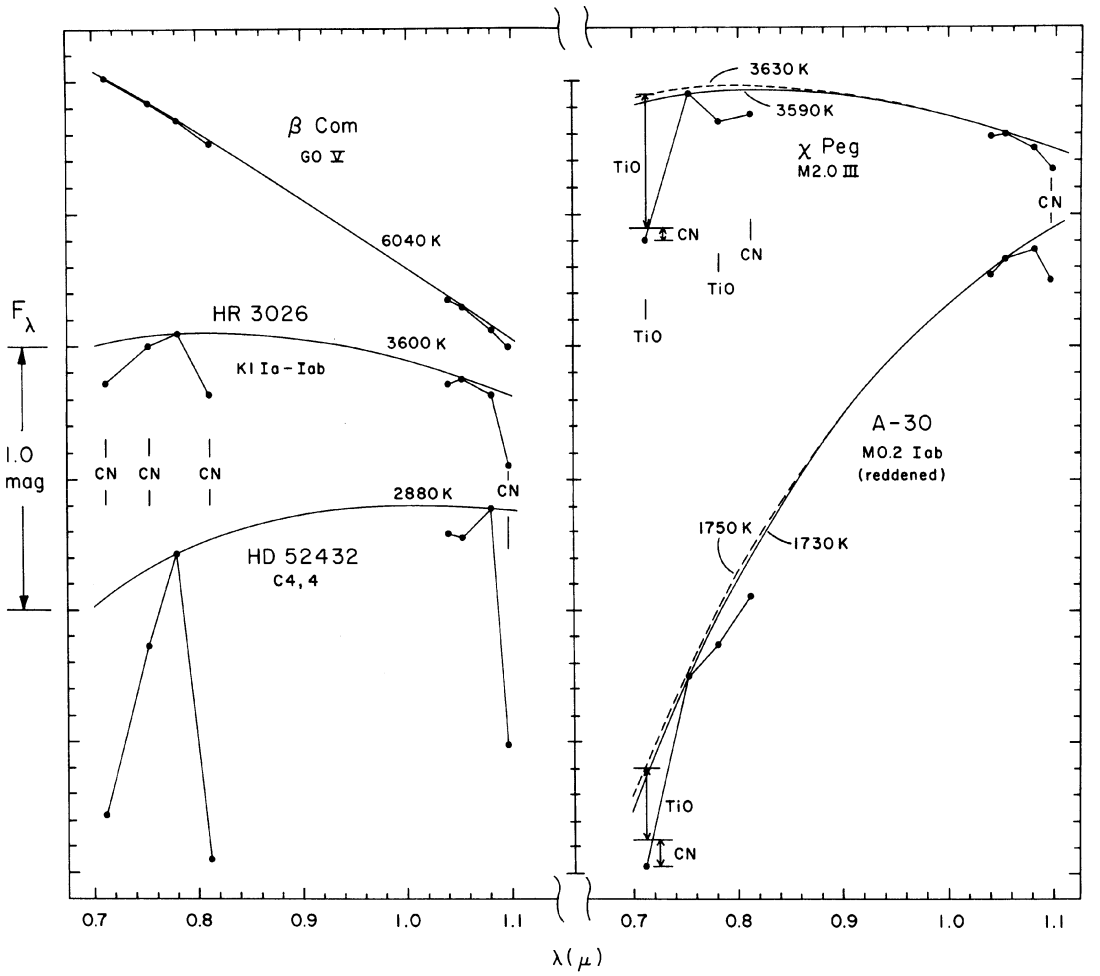

FIG. 1. Spectra of representative stars on the eight-color system. Flux per unit wavelength interval, expressed in magnitudes with an arbitrary zero point for each star, is plotted against wavelength in microns. On the left are three stars with CN absorption but no TiO: β Com (G0 V), HR 3026 (K1 Ia-Iab), and HD 52432 (C4,4). On the right are two M stars: χ Peg, a normal M2 giant, and A-30, a heavily reddened supergiant discovered in this study. Each dataset has been fitted by a blackbody continuum and the corresponding temperature is indicated. For the M stars the continuum is shown both before and after correction for CN absorption in filter 2, and the portion of the depression in filter 1 that is attributable to CN is indicated.

curve is the color temperature T_c of the star. In Fig. 1 the values found for T_c are indicated, and except for the two supergiants, both of which are reddened, they fall in the expected ranges for their spectral types. Detailed comparisons with model-atmosphere energy distributions (Wing *et al.* 1985) have shown that the color temperatures found in this way for G, K, and early M stars are about 200 K lower than the stellar effective temperatures as a result of the distortion of the continuum by H^- opacity.

We will often use the reciprocal color temperature $\theta_c = 5040/T_c$ as our index of continuum color. This quantity behaves like a conventional color index (magnitude difference)—in fact, the color indices of blackbodies are directly proportional to θ_c except at very high temperatures which are not of interest in this program—and has the added advantage that it is independent of the particular wavelengths used in its determination. Thus we can use different continuum points for M stars and carbon stars and still compare their color temperatures directly.

We define the "depression" in any filter as the difference between the observed magnitude and that of the blackbody continuum, and we designate by D1, D2,..., the depressions in filters 1, 2, and so on. These depressions, expressed in magnitude units, are indices of the amount of absorption in each filter and, like spectroscopic equivalent widths, they are independent of reddening because they are referred to the continuum at the same wavelength. They will be used to define indices of TiO and CN strength, which in turn form the basis of our two-dimensional spectral classification. Unlike the reddening-free indices of other photometric systems which involve complicated algebraic combinations of the observed magnitudes and numerical coefficients adjusted on the basis of an assumed interstellar reddening law, our reddening-free indices are defined by a procedure which is easy to visualize in terms of spectro-

scopic concepts, but which can be employed only because our data are absolutely calibrated.

To extract the maximum information from the photometric data, we require indices of the three intrinsic variables—temperature, TiO strength, and CN strength—that are as sensitive as possible to the variable in question, and yet independent of each other. The sensitivity of the observed color temperature to the effective temperature of the star is assured by requiring the use of widely spaced continuum points. To make the color temperature independent of band strength we must use good continuum points and be prepared to apply corrections for residual absorption within the bandpasses of continuum filters (see below). The sensitivity of the band-strength indices is maximized by using the strongest band of each molecule. Our indices of TiO and CN are independent of the slope of the continuum (and hence independent of both the star's intrinsic color and the interstellar reddening) since they are based on depressions measured with respect to the continuum, as discussed above.

The problem that remains is to make the indices of TiO and CN independent of one another. This is not trivial because both molecules have extensive, overlapping band systems throughout the near infrared. At the same time it is important to achieve this independence, since our two-dimensional classification is based on the strengths of TiO and CN and implicitly assumes that our indices measure two independent quantities.

Let us look again at the eight-color spectra plotted in Fig. 1. There is no problem in defining the long-wavelength end of the continuum since filters 5–7 are all satisfactorily close to the true continuum in K and M stars (until type M6, when VO appears). The short-wavelength continuum point, however, necessarily changes with spectral type. The stars shown in the left half of the figure are free of TiO, and the absorptions seen in their eight-color spectra are almost entirely due to the effects of CN. (In the G-type dwarf, the depression of 0.01 mag at filter 4 may be attributed to CN, to judge from the solar spectrum, but the larger depression of 0.04 mag at filter 8 is mostly due to the hydrogen line $P\gamma$ in the wing of the filter bandpass.) In stars of these types, filter 3—which falls at a minimum of CN opacity just shortward of the strong (2,0) bandhead—is always used as the shortward continuum point since filters 1, 2, and 4 are all measurably affected by CN. In the M stars shown in the right half of the figure, the effect of CN can still be seen at filters 4 and 8, but now we also see strong TiO bands in filters 1 and 3. Consequently, filter 2 takes over the role as the best shortward continuum point, although clearly it must still be affected by CN.

From observations of stars with CN only, we find that the absorption due to CN in filters 1 and 2 can be adequately represented as being simply proportional to the strengths of the stronger CN bands in filters 4 and 8. If we define our CN index, i(CN), as the average of the depressions in filters 4 and 8, viz.

$$\mathrm{i(CN)} = 0.5\ (\mathrm{D4} + \mathrm{D8}), \tag{1}$$

then the depressions at filters 1 and 2 due to CN are

$$\mathrm{D1(CN)} = 0.55\ \mathrm{i(CN)} \tag{2}$$

and

$$\mathrm{D2(CN)} = 0.20\ \mathrm{i(CN)} \tag{3}$$

respectively. Expressions (2) and (3) give the corrections (in mag) to be applied to the fluxes in filters 1 and 2 to remove, approximately, the effects of CN absorption. A new blackbody fit employing the corrected flux in filter 2 then provides an improved (higher) value for the color temperature. Finally, the TiO index is defined simply as the depression in filter 1:

$$\mathrm{i(TiO)} = \mathrm{D1} \tag{4}$$

obtained after CN corrections have been applied to both filters 1 and 2.

The effects of these corrections are illustrated in Fig. 1. In χ Peg, an ordinary class III giant, the original blackbody fit (continuous curve) yields $T_c = 3590$ K and i(CN) $= 0.086$ mag, implying corrections of 0.047 and 0.017 mag at filters 1 and 2, respectively. The final blackbody continuum (dashed curve) thus passes 0.017 mag above the measured flux in filter 2 and corresponds to a temperature 40 K higher. Since the final CN index, 0.091, has hardly been changed by the correction procedure, no further iteration is necessary. The index i(TiO) is decreased from 0.520 to 0.493 mag by the corrections, and the spectral type, according to the calibration given below, is reduced from M2.1 to M2.0.

Clearly, the effects of the corrections for CN in filters 1 and 2 are so small in ordinary giants like χ Peg that they could as well be neglected. In supergiants, however, the CN absorption is two to three times as great as in giants, and the corrections become significant. In the case of A-30 shown in Fig. 1, the change in the blackbody continuum is hard to see because the slope is so steep, but the spectral type is changed from M0.8 to M0.2. If we did not correct the data for supergiants, we would assign them color temperatures that are systematically low relative to the giant scale and spectral types that are $\sim$0.5 subtype later than those assigned to giants of the same TiO strength. For consistency, we apply the corrections to stars of all luminosity classes.

Note that these corrections are not needed for stars which do not have TiO absorption, since then the corrected flux in filter 2 should define the same continuum as does the observed flux in filter 3 used for the first blackbody fit. In such cases we simply adopt the results of the first fit. Also, in spectra later than M6 this correction procedure becomes ineffective because VO bands appear in filter 2 and grow rapidly with decreasing temperature. However, in the interval K4–M6 which includes most of the stars observed in this program, we believe that the procedure described here provides the best indices of TiO and CN strength that can be obtained from our data.

In summary, we use a two-step procedure to obtain indices of the strengths of TiO and CN that are independent of each other. First, a blackbody curve is found that passes through the best continuum point in each of the two

groups of filters. This continuum is used to define initial values of D4 and D8, and hence of i(CN). Corrections for CN contamination in filters 1 and 2 are then computed and applied to the fluxes at these wavelengths. A second blackbody fit is then carried out to obtain final values for θ_c, i(TiO), and i(CN). If the final conclusion is that no TiO is present (i.e., if all the absorption at filter 1 can be attributed to CN), then the spectral type is earlier than K4.0 and the values of θ_c and i(CN) from the first blackbody fit are retained as the final values.

3.5 Two-Dimensional Spectral Classification

It is by a fortunate accident of nature that the two molecules whose band systems dominate the near-infrared spectra of late-type stars behave so differently with respect to the physical variables, temperature and gas pressure. The eight-color photometry takes advantage of this accident to give two-dimensional (temperature/luminosity) classifications on the basis of its measurements of TiO and CN strength (Wing & White 1978).

The temperature sensitivity of TiO is so pronounced that it has always been used as the primary basis for dividing M stars into subtypes. That the TiO strength is nearly independent of luminosity is shown by the fact that the relation between spectral type (i.e., TiO strength) and temperature (or color) is at least approximately the same for dwarfs, giants, and supergiants despite their enormous difference in luminosity. The positive luminosity effect of CN discovered by Lindblad (1922) has often been used in low-resolution surveys for luminous stars, but it has been relegated to a secondary role in the luminosity classification of late type stars on the MK system (Keenan 1963) in favor of atomic-line ratios, which are less likely to be affected by composition differences. Griffin & Redman (1960), who measured the CN band at 4215 Å photoelectrically, showed that the mean relation between CN strength and spectral type within each luminosity class is quite flat; that is, the CN strength depends only weakly upon the temperature. The bands of the Violet System do appear to weaken in late K stars, and Griffin & Redman were not able to measure CN in M stars. The weakening of the Violet System is, however, an opacity effect, and Wing (1967b) has found that the bands of the Red System in the near infrared can be measured in M type giants and supergiants, although only the (0,0) band near 11 000 Å remains uncontaminated in the mid and late M types. It appears, in fact, that the mean relation between the strength of the CN Red System (0,0) band and the temperature, at any luminosity, is quite flat throughout the K and M types.

Of course, the column density of any molecule must depend to some extent on both the temperature and the gas pressure. But since it has not been possible to establish any real temperature dependence of the CN strength or luminosity effect for TiO, we will accept the TiO and CN strengths as pure indicators of temperature and luminosity, respectively. In the previous section we discussed the observational problem of defining indices of TiO and CN strength that are independent of each other. Now, to use these indices for classification, we simply need to calibrate them in terms of spectral type and luminosity class.

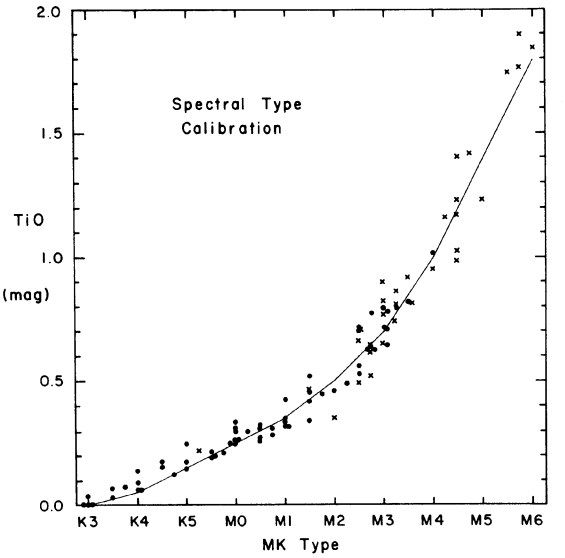

FIG. 2. Calibration of the TiO index. TiO is the depression (in mag) at filter 1 (7120 Å) caused by the $\gamma(0,0)$ band of TiO, after correction for contamination by CN. The MK type is from Keenan & McNeil (1989); variables with amplitudes of 0.1 mag or more are plotted as crosses (×). The adopted calibration consists of a series of straight-line segments.

To calibrate the index i(TiO), we have used eight-color observations of stars that have been classified spectroscopically as luminosity class III giants on the MK system, and to ensure the homogeneity of the calibration data we have used only stars classified by P. C. Keenan. The photometry of these bright stars has been collected over a period of time with S-1 photocells at various small telescopes at KPNO, CTIO, and Lowell Observatory.

In Fig. 2 our CN-corrected TiO index is plotted against spectral type on the MK system for 92 K3–M6 stars classified as class III giants by Keenan & McNeil (1989). We have rejected stars with significant spectral peculiarities and variables which have shown obvious changes in spectral type, although it has been necessary to use small-range variables to define the calibration of the later types. Known (i.e., designated) variables are plotted as crosses unless their catalogued amplitudes are less than 0.1 mag, and it is likely that several of the other stars also vary appreciably. All stars plotted have at least two accordant photometric observations, and the index i(TiO) has been determined from the averaged data. Also, 71 of the stars (77% of those plotted) appear in Keenan & McNeil (1989) with daggers before their names to indicate that they have been recommended for use as standards by Keenan & Yorka (1988). In plotting the MK types we have followed the recommendations of Keenan and McNeil: namely, the spectroscopic subdivisions M0, M0+, M0.5, M1−, M1,... are considered to divide each subtype into four equal parts, and the inter-

TABLE 5. Calibration of the eight-color TiO index.

Spectral Type	TiO (mag)	Spectral Type	TiO (mag)
K4.0	0.05	M2.5	0.60
K4.5	0.10	M3.0	0.70
K5.0	0.15	M3.5	0.85
K5.5	0.20	M4.0	1.00
M0.0	0.25	M4.5	1.20
M0.5	0.30	M5.0	1.40
M1.0	0.35	M5.5	1.60
M1.5	0.42	M6.0	1.80
M2.0	0.50		

val from K5 to M0 is considered to be the same size as the other subtype intervals.

The adopted calibration consists of a series of straight-line segments, as shown in Fig. 2 and tabulated in Table 5. This calibration has not changed since the work of White & Wing (1978), although it is now based on a larger number of standards. Spectral types measured on the eight-color system are expressed with decimal subdivisions and are easily distinguished from MK types with their plus and minus signs. Note that type M0.0 immediately follows type K5.9.

The photometric errors in i(TiO) are generally somewhat less than 0.01 mag, which corresponds to exactly 0.1 subtype throughout the interval K4.0–M1.0. At later types the relation becomes progressively steeper, and in the interval M4–M6 an error of 0.01 mag in i(TiO) corresponds to an error of only 0.025 in spectral type.

Some of the scattering Fig. 2 is no doubt due to variability, and some is due to the fact that TiO strength is not the only criterion considered when MK types are assigned. The largest discordances in Fig. 2 amount to 1.0 subtype (e.g., the difference between M0.0 and M1.0) and, as Wing & Yorka (1979) have already shown, the mean deviation between eight-color and MK types for standard stars classified by Keenan is 0.3 subtype, barely larger than the stated resolution of the MK system (one-quarter subtype). The eight-color data have proven useful in evaluating the internal consistency of the spectral types for M stars obtained by various methods, as well as in revealing systematic differences between data sets (Wing & Yorka 1979).

One of the original objectives of the eight-color photometry was to unify the classification scales of M type dwarfs, giants, and supergiants by assigning the same type to all stars of the same TiO strength, regardless of their luminosity class (Wing 1973). Thus the calibration given in Table 5 is used for stars of all luminosities. Note that the CN corrections discussed in the previous section are needed to make the spectral-type scales the same for all luminosity classes, since stars of different luminosities have systematically different CN strengths.

The special problems of classifying stars later than M6 will not be considered here because such stars are recognizable on our objective-prism survey plates and have been excluded by the selection criteria. Although supergiants of very late type are known to exist (Lockwood & Wing 1982), it is clear that the great majority of late M stars are ordinary giants of little value to a galactic-structure project: it is not even possible to determine the reddening of late M stars accurately since they do not follow well-defined relations between band strength and intrinsic color. The interested reader will find discussions of the photometric classification of very late M stars in Wing & Lockwood (1973) and in Lockwood & Wing (1982).

TABLE 6. Calibration of CN index.*

Luminosity Class	Range in CN
Ia	≥ 0.245
Ia-	0.235 - 0.244
Iab	0.185 - 0.234
Iab-	0.175 - 0.184
Ib	0.125 - 0.174
Ib-	0.115 - 0.124
II	0.095 - 0.114
III	0.035 - 0.094
V	≤ 0.034

*Valid for types K4 - M4.

The calibration of the index i(CN) in terms of luminosity class is given in Table 6. It is taken from White & Wing (1978), except that the indices in that paper are expressed in units of 0.01 mag instead of magnitudes. The boundaries of the intervals in i(CN) were chosen to maximize the agreement with luminosity classes of MK standards of types K4–M4. The calibration is probably also valid somewhat outside this range; in G stars, however, the calibration indicates only a lower limit to the luminosity since the CN strength weakens rapidly with increasing temperature as a result of increased molecular dissociation.

It should be emphasized that luminosity classes on the eight-color system are not MK classes. In fact, the eight-color and MK luminosity classes are based on such totally different criteria—absolute strength of CN versus ratios of atomic lines—that they might better be considered independent quantities. Nevertheless, the eight-color and MK luminosity classes are in excellent agreement as regards not only the distinction between dwarfs, giants, and supergiants but also the subdivision of supergiants into classes Ia, Iab, and Ib. On the other hand, the agreement breaks down if we try to subdivide the class III giants: these stars have a wide enough range of CN strength (see Table 6) that a subdivision would be observationally pos-

sible, but the giants of MK class IIIa do not have systematically stronger CN than class IIIb giants. For the class III (and probably class II) giants, we believe that the MK luminosity subdivisions are more likely to reflect true differences in luminosity, and that discordant CN strengths should be looked upon as evidence of composition differences (Wing 1989a). For this reason we prefer not to assign luminosity subdivisions to class II and III giants on the eight-color system.

In the present study we need to distinguish the true supergiants from stars of lower luminosity, and we would like to subdivide the supergiants as finely as possible in order to improve the accuracy of our distance estimates. For these purposes the strength of CN seems to be as reliable a luminosity indicator as any atomic line ratio available in M stars, probably because the supergiants are all of a young population and are nearly homogeneous in composition. Of course, the CN bands have the additional advantage that they are broad features, permitting the use of narrowband photometry and hence the classification of distant stars with small telescopes.

In Sec. 4 below, we discuss luminosity classifications obtained from our CCD spectra from the strength of lines of the Ca II infrared triplet. Because of the possibility of composition differences among the stars studied, and because CN may be particularly sensitive to such composition differences, we consider it important to obtain an independent estimate of the luminosity based on atomic line strengths. At this point in our study we do not know which of our luminosity criteria, CN or Ca II, will prove the more reliable as a distance indicator for red supergiants. The preliminary indications are that the two criteria are quite well correlated, although both become more difficult to use in stars later than about M2, whose near-infrared spectra are dominated by TiO bands.

3.6 Determination of Interstellar Reddening and Distance

In order to determine distances from our photometric data, we need a calibration of the luminosity classes (or of the luminosity criterion itself) in terms of the absolute magnitude at one of the observed wavelengths, and a determination of the interstellar absorption at the same wavelength. The latter can be inferred—by assuming a standard interstellar reddening law—from the measured reddening, which in turn is found by comparing the observed color to the intrinsic color corresponding to the observed spectral type.

Clearly, the process of determining distances from photometric data requires a knowledge of the intrinsic properties of the stars used. For red supergiants these properties are not well known, and we must rely upon our own ongoing efforts to determine their intrinsic colors and absolute magnitudes. Here we can present only a progress report. By obtaining eight-color photometry for M-type supergiants belonging to clusters and associations whose distance and reddening are known (usually from *UBV* photometry), we can in principle find the intrinsic colors and absolute infrared magnitudes of the red supergiants. In this way we obtain the necessary relations between intrinsic color and spectral type, and between absolute infrared magnitude and CN index. We use the magnitude at filter 5 ($\lambda_c = 10\,395$ Å) for these computations because it is nearly free of blanketing in almost all spectral types; the apparent magnitude in this filter is designated $I(104)$ and the corresponding absolute magnitude $M(104)$.

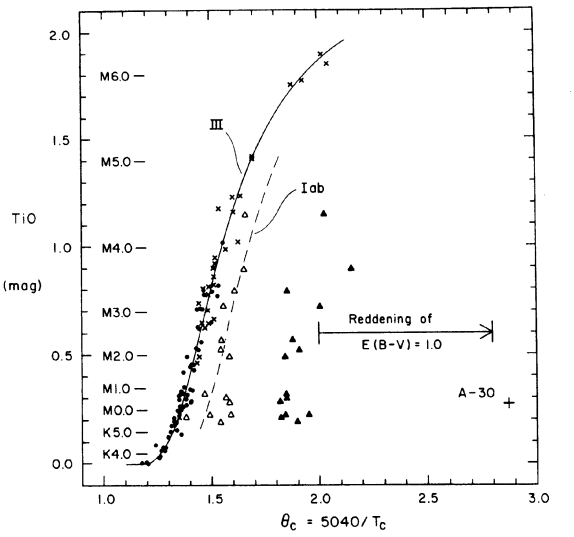

FIG. 3. Relation between the index i(TiO) (calibrated in terms of spectral type) and the reciprocal color temperature θ_c. Nearby giant stars (dots, or crosses if variable with amplitudes $\geqslant$0.1 mag) define the intrinsic luminosity class III relation (see Table 7). Supergiants in or near the Double Cluster in Perseus (filled triangles: as observed; open triangles: after correction for reddening) define the intrinsic class Iab relation. Reddening affects only the horizontal axis; the length of the arrow shows the effect of reddening amounting to $E(B-V)=1.0$ mag. The heavily reddened supergiant A-30 (see spectrum in Fig. 1) lies near the right edge of the figure.

Unfortunately, determinations of distance and reddening are never simple, even for well-defined star clusters. When clusters have been studied by different authors, the results for distance and reddening are often significantly different. In addition we must contend with the question of the cluster membership of individual red supergiants, especially in the case of loosely defined associations and in directions where we may be seeing clusters at different distances along the same line of sight. Thus each case must be treated individually and value judgments made. Our work on this problem will be discussed in a separate paper of this series.

For normal luminosity class III giants, the relation between intrinsic color and spectral type is easily determined because there are many such stars close enough to the Sun to be unreddened. Figure 3 is a plot of the TiO index measured by filter 1 versus the reciprocal color temperature $\theta_c = 5040/T_c$, corrected for the effect of CN in filter 2 as discussed in Sec. *3.4*; the calibration of i(TiO) in terms of spectral type is also indicated. The stars plotted are the same ones that were used in Fig. 2 to define the spectral-type calibration; namely, they are bright, normal, luminos-

ity class III giants classified by Keenan & McNeil (1989) with two or more accordant photometric observations; again variables with cataloged amplitudes of 0.1 mag or more are distinguished by crosses. The hand-drawn continuous curve passing through the points (both dots and crosses) is taken to be the intrinsic relation between band strength and θ_c.

The effect of interstellar reddening, which makes θ_c larger without changing i(TiO), is to move stars horizontally to the right in Fig. 3. Since the scatter among the points representing the giants is much larger than the observational errors (which are approximately the size of the dots), we must consider whether it could be caused by small amounts of interstellar reddening, in which case the blue-side envelope of the points would be a better estimate of the intrinsic relation. However, since all of the stars plotted are bright enough to be included in the *Bright Star Catalogue* and, if correctly classified as normal giants, are within about 200 pc of the Sun, we can be confident that nearly all of them are free of reddening. We therefore must attribute the general scatter to another source, most likely composition differences which affect the TiO band strength at a given temperature, and we have taken the mean relation to represent the intrinsic one.

It is reasonable to expect that supergiants obey a different relation between band strength and intrinsic color since, with different gas pressures and different concentrations of H^- and other continuous opacity sources, they are likely to have different TiO column densities at a given effective temperature. A preliminary attempt to determine the supergiant relation has been made on the basis of 14 red supergiants of class Iab in or near the Double Cluster in Perseus. The filled triangles in Fig. 3 represent the observed colors and band strengths of these stars, from White & Wing (1978); they are displaced to the right of the giant relation by about 0.4 in θ_c, on the average, largely as a result of interstellar reddening. These stars can be unreddened individually using the color excesses $E(B-V)$ found by Wildey (1964) from faint stars of earlier type in the vicinity of each, and the relation

$$\Delta\theta_c = 0.80E(B-V) \tag{5}$$

(Wing 1967b). The unreddened data points, plotted as open triangles, all lie to the right of the giant relation, and if there has been no systematic underestimate in Wildey's color excesses they indicate that the intrinsic relation for supergiants of class Iab is displaced by about 0.12 in θ_c to the right of the giant relation. The two relations are given in tabular form in Table 7. The giant relation may be regarded as definitive, and until a better determination for supergiants becomes available, we will use the provisional relation given in the table. We will also provisionally use the class Iab relation for supergiants of all subtypes.

We have adopted "van de Hulst curve No. 15" (Johnson 1968) as a good representation of the normal interstellar reddening law; it has the property that the ratio of total to selective absorption, $A_V/E(B-V)$, is 3.05. From this curve we find that the absorption at 10 400 Å, $A(104)$, is related to the color excess in $B-V$ in the following simple manner:

$$A(104) = 1.0E(B-V), \tag{6}$$

or, from relation (5),

$$A(104) = 1.25\Delta\theta_c, \tag{7}$$

where $\Delta\theta_c$ is the star's horizontal displacement from the appropriate intrinsic relation in Fig. 3.

TABLE 7. Intrinsic colors.

TiO	Spectral Type	θ_c (intrinsic) III	Iab
0.05	K4.0	1.268	-
0.10	K4.5	1.300	-
0.15	K5.0	1.319	1.439
0.20	K5.5	1.336	1.456
0.25	M0.0	1.353	1.473
0.30	M0.5	1.370	1.490
0.35	M1.0	1.385	1.505
0.40	M1.3	1.400	1.520
0.45	M1.8	1.413	1.533
0.50	M2.0	1.425	1.545
0.60	M2.5	1.450	1.570
0.70	M3.0	1.475	1.595
0.80	M3.3	1.500	1.620
0.90	M3.7	1.527	1.647
1.00	M4.0	1.555	1.675
1.10	M4.3	1.583	1.703
1.20	M4.5	1.613	1.733
1.30	M4.8	1.650	1.770
1.40	M5.0	1.690	1.810
1.50	M5.3	1.740	-
1.60	M5.5	1.795	-
1.70	M5.8	1.855	-
1.80	M6.0	1.934	-
1.90	-	2.045	-
2.00	-	2.200:	-

We are attempting to obtain absolute $M(104)$ magnitudes for a large enough number of supergiants belonging to clusters and associations to be able to calibrate the CN index directly in terms of absolute magnitude. This will avoid the quantization imposed by grouping stars rather artificially into luminosity classes. For the time being, however, we adopt the simple calibration of the luminosity subtypes given in Table 8. The values of $M(104)$ given for giants have been obtained by applying the $V-I(104)$ colors tabulated as a function of spectral type by Wing (1967b) to the absolute magnitudes M_V given by Egret *et al.* (1982). For the supergiants of class Iab we have again used stars associated with the Double Cluster observed on the eight-color system by White & Wing (1978); we have followed the procedure outlined above to correct the observed $I(104)$ magnitudes for interstellar absorption and have assumed a distance modulus of 12.0 mag (Schild 1967). We do not have independently determined se-

TABLE 8. Absolute $M(104)$ magnitudes.

Type	Luminosity Class			
	III	Ib	Iab	Ia
K4	-2.4			
K5	-2.9		-7.8	
M0	-3.4	-7.2	-8.0	-9.4
M1	-3.8		-8.2	
M2	-4.2	-7.6	-8.4	-9.8
M3	-4.6		-8.6	
M4	-5.0	-7.9	-8.7	-10.1
M5	-5.5:		-8.8:	

quences for classes Ia and Ib; for these stars we have simply assumed that the differences in absolute magnitude between classes Ia, Iab, and Ib at a given spectral type are the same in $M(104)$ as Blaauw (1963) has given for M_V. While the values given in Table 8 must be regarded as preliminary, they are believed to be adequate to give realistic estimates of supergiant distances.

The determination of the distance of an M star observed on the eight-color system proceeds as follows. A blackbody curve is fitted to the reduced fluxes, corrected for CN contamination at filters 1 and 2 according to relations (1) and (2), to determine the color temperature T_c (or its reciprocal $\theta_c = 5040/T_c$) and indices of TiO and CN strength. The spectral type and luminosity class are obtained from the calibration of these indices (Tables 5 and 6). The reddening $\Delta\theta_c$ is next found by comparing the observed color θ_c to the intrinsic color corresponding to the star's TiO index and luminosity class (Table 7), and the absorption $A(104)$ is obtained from relation (7). With the absolute magnitude $M(104)$ obtained from the two-dimensional classification by interpolation in Table 8, the true distance modulus is found from

$$(m-M)_0 = I(104) - A(104) - M(104). \quad (8)$$

The distance d itself, in parsecs, is then found from

$$(m-M)_0 = 5 \log d - 5. \quad (9)$$

As an example of this procedure, let us find the distance of the reddened supergiant A-30 whose eight-color spectrum is shown in Fig. 1. This star is classified M0.2 Iab from its indices i(TiO) and i(CN), and its observed reciprocal color temperature is $\theta_c = 2.873$, placing it near the right-hand edge of Fig. 3. The intrinsic color for M0.2 Iab stars is $\theta_c = 1.480$ (Table 7), so that the reddening is $\Delta\theta_c = 1.393$ and the absorption is $A(104) = 1.741$. Since the observed magnitude in filter 5 is $I(104) = 8.328$, the corrected apparent magnitude is 6.59. With $M(104) = -8.04$ from Table 8, the distance modulus is found to be 14.63 and the distance $d = 8.4$ kpc. This star lies in the constellation Carina but is clearly at a much greater distance than familiar objects such as η Car ($d \sim 1.9$ kpc) or NGC 3293 ($d \sim 2.6$ kpc), as indeed we might have anticipated from its heavy reddening. Galactic-structure maps show a "Sagittarius-Carina Arm" extending away from the Sun in the direction of this star, but very little information is available about specific objects more distant than 3 of 4 kpc. Since A-30 is comfortably brighter than the limiting magnitude of our survey and also is not as luminous as some stars we have found, it is clear that our method is capable of reaching supergiants at still greater distances.

The main source of error in such distance determinations is the uncertainty in the values of $M(104)$ assigned on the basis of CN strength. We are not yet able to evaluate the quality of CN as a luminosity indicator, i.e., the extent to which the CN strength may depend upon quantities other than the luminosity. As mentioned earlier, our evaluation of the intrinsic spread in the $i(CN) - M(104)$ relation will be based on supergiants belonging to clusters and associations. In any event, our method has two important advantages over conventional distance determinations for M stars based on *UBV* photometry and tabulated values of M_V: (1) the absorption in $I(104)$ is only one-third as great as in V, and (2) the $M(104)$ magnitude should be a better-defined quantity than M_V for M stars since it is measured much closer to the peak of the energy distribution and is unaffected by TiO absorption. Hence there is reason to expect that our distances will be more accurate than those available for M supergiants in the past. This advantage is, of course, in addition to those realized from the increased numbers and greater distances of the supergiants found in this project.

4. NEAR-INFRARED SPECTROSCOPY OF SUSPECTED LATE TYPE SUPERGIANTS

4.1 Observations and Reductions

Spectra of many of the candidate stars are taken in the near-infrared region after they are observed on the eight-color system. The near-infrared is used to take advantage of the great sensitivity of CCD detectors and the brightness of late type stars in this region. The spectra serve as a check on the photometric classification and enable us to identify various kinds of peculiar stars (e.g., S stars) that might not be recognizable from the photometry and to classify stars that lie outside the range of applicability of the eight-color system (e.g., reddened supergiants earlier than K4). The wavelength range 6400–8800 Å was chosen so as to include the ZrO band of S stars at 6474 Å and the Ca II triplet which is sensitive to luminosity at a given temperature class. Our desire to record this range in a single observation dictated the choice of grating and order and hence of pixel resolution at a given telescope.

The spectra taken to date have been obtained in several runs at the CTIO 1.5 m, one run at the Yale 1.0 m at CTIO (both at resolutions of 4 Å/pixel), and one at the DuPont 2.5 m telescope at Las Campanas (3 Å/pixel). At CTIO, the Cassegrain spectrograph was used with a 300 lines/mm grating, a 160 mm camera, and a GEC 576×385 CCD with 22 μm pixels, while at LCO the modular spectrograph

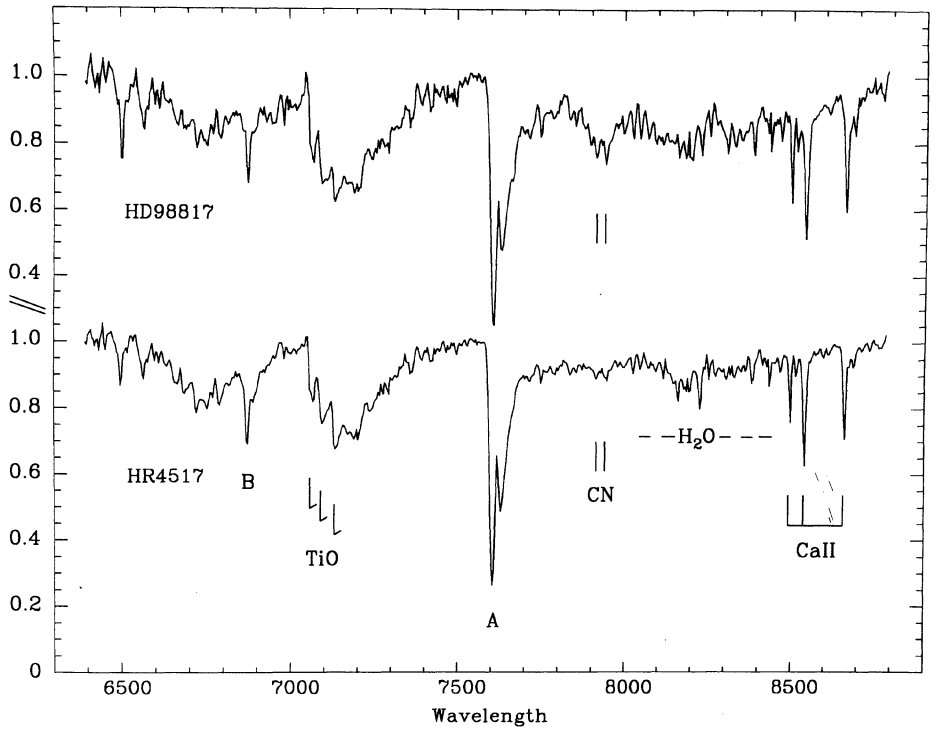

FIG. 4. Luminosity effects at spectral type M1. Flattened CCD spectra at 4 Å/pixel resolution are shown for the MK standards HD 98817 (M1 Iab-Ib) and HR 4517 ($=\nu$ Vir; M1 III, weak CN). The triple-headed TiO band near 7100 Å, which is also measured by the eight-color photometry and is used to assign temperature classes, has the same strength in the two spectra. Note the differences in the luminosity-sensitive features: CN, especially near 7900 Å, and the Ca II triplet. The atmospheric A and B bands of O_2 and a region affected by telluric H_2O lines are also indicated.

was employed with a 600 lines/mm grating, an 85 mm camera, and a TI 800×800 chip with 15 μm pixels.

Multiple unsaturated exposures are taken of each candidate star and classification standard star (Keenan & McNeil 1989) and are averaged before flatfielding, bias subtraction, and spectrum extraction following the standard procedures of the IRAF reduction packages. A total of about 80 MK standards later than G0 and of luminosity class III or brighter have been observed on this program, with at least 40 observed on each run in addition to a few flux standards per night. We insert neutral-density filters to avoid saturation for the brightest standards. All spectra are flux and wavelength calibrated using normal IRAF procedures. We normally have not observed enough extinction stars to be able to remove telluric features with confidence, but this is of little consequence in classifying the spectra.

4.2 Spectral Classification

Because of the great differences in spectral slope between our program stars, many of which are heavily reddened, and the standards, all spectra are flattened before classification is attempted. This is accomplished by passing a Legendre polynomial of order 3 through the best continuum points and dividing the spectrum by that fit.

The luminosity criteria in the near infrared that can be employed at our resolution include the CN features at 7916/7941 Å (Sharpless 1956; Schulte-Ladbeck 1988) and the lines of the Ca II triplet at 8498, 8542, and 8662 Å (Merrill 1934; Jones *et al.* 1984). The CN features are bandheads at the start of the $\Delta v=+2$ sequence, which is also measured near 8120 Å on the eight-color photometric system; the Ca II features, on the other hand, provide information that is independent of the photometry. Both the CN bands and the Ca II lines strengthen with increasing luminosity at a given spectral type. Figure 4 presents the flattened spectra of the M1 standards HD 98817 (luminosity class Iab-Ib) and ν Vir (HR 4517, a weak-CN class III giant). The differences in the luminosity-sensitive features are clearly seen, although they probably are not due entirely to luminosity differences in this case as ν Vir appears to be metal poor. Since these features—especially the Ca II triplet—are also sensitive to temperature, our procedure is to compare program stars to MK standards of the same eight-color temperature type, as judged by the TiO absorption at 7120 Å.

Figure 5 shows the flux-calibrated spectrum of the program star X-46 ($\alpha=7{:}31{:}53.0$, $\delta=-22{:}33{:}02$, 1950) both before and after flattening by the procedure described above. The wavelength regions used for fitting the continuum are indicated. This star is rather heavily reddened and

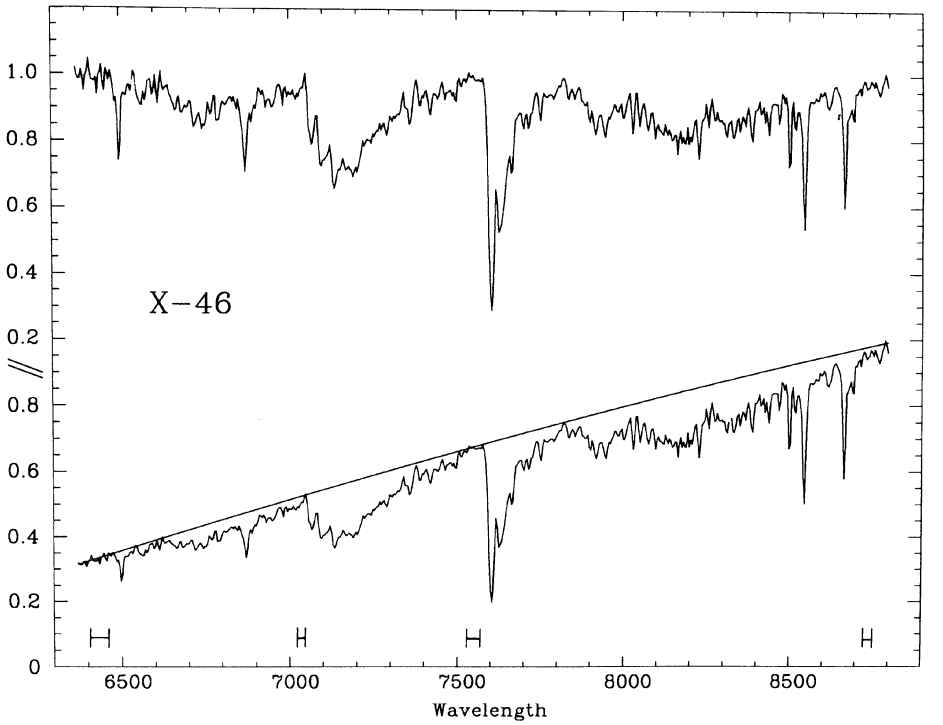

FIG. 5. Spectrum of the reddened program star X-46. Below is the observed, flux-calibrated spectrum; the same spectrum after flattening is shown above. The continuum fit used to flatten the spectrum is shown, and the wavelength regions used to determine the continuum are indicated at the bottom. From comparison of the flattened spectrum with those of the standards in Fig. 4, the star is classified M1 Ib.

its observed spectrum slopes upward toward longer wavelengths; unreddened classification standards of this temperature class are nearly flat. By flattening the spectra of all stars it is easier to make fair comparisons of feature strengths in program stars and standards. Comparison of the spectrum of X-46 with those of the standards shown in Fig. 4 indicates a type of about M1 Ib, in good agreement with its eight-color type of M0.2 Ib.

The assignment of luminosity classes is done at the computer screen using a feature of IRAF which permits comparison of a program star and several standard stars at once. To avoid uncertainties caused by differences in resolution, we try to compare program stars to standards taken on the same run, but this constraint has sometimes been relaxed in order to draw upon a larger set of standards.

We considered two different approaches to the assignment of luminosity classes from our spectra. The first is the comparison of the entire recorded spectra of a program star and a set of standards, looking simultaneously at several features and also judging which standard gives the best overall match. This is the traditional classification procedure recommended by Morgan and Keenan for the MK system, and it may be considered to give the "best" classification that can be obtained from the data because it makes use of all the information available. However, when applied to late type supergiants in the near infrared, this method gives results that are strongly influenced by the CN strength. This is because the CN bands, while not individually conspicuous, are distributed throughout the near infrared and are strong enough in supergiants to affect the appearance of the spectrum, at least in types earlier than about M2. Since in this project we have CN-based luminosity classifications from the photometry, it is not very useful to obtain redundant information from the spectra; it is more helpful to use the spectra to obtain luminosity classes on the basis of the Ca II lines which can serve as an independent check on the quality of our photometric luminosities. We have therefore adopted a second approach, that of using *only* the Ca II lines in assigning our spectroscopic luminosity classes. To make the classifications as independent of CN as possible, we plot only the region of the Ca II lines, on an expanded scale, when making these judgments. The classifications are based on the depths and overall appearance of the Ca II lines in the normalized, flattened spectra of program stars and standards.

We have also experimented with a numerical technique, using equivalent widths of the Ca II lines instead of their depths. Both methods are somewhat subjective, depending as they do upon the adopted continuum level. We find that the results from these two procedures are well correlated for the K stars but show less good agreement in M stars as strengthening absorption by the 8432 Å band of TiO destroys the continuum in the Ca II region. The use of equivalent widths has been discussed further in MacConnell *et al.* (1987), where we have also shown examples of unflat-

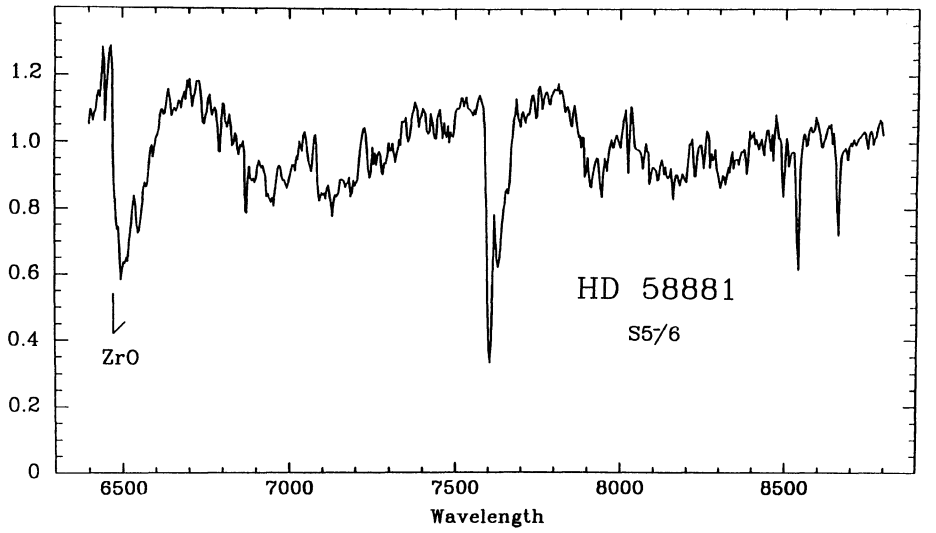

FIG. 6. Flattened spectrum of the S star HD 58881 (S5-/6). Note the strong 6474 Å band of ZrO, the defining characteristic of S stars, and the absorptions due to CN in the 6800–7400 and 7800–8400 Å regions. This star displays no TiO.

tened spectra of standard and program stars.

In a later paper we will discuss the degree of correspondence we find between our CN-based photometric and Ca II-based spectroscopic luminosity classes. The preliminary indications are that the two are well enough correlated that we will be able to publish a single-luminosity classification for supergiants, noting discrepancies in individual cases.

4.3 Stars of Unusual Types

Stars of type S are often difficult to distinguish from M supergiants because they display several of the same spectral characteristics. This is particularly the case in the near infrared, since the ZrO molecule—the presence of which is generally considered the defining characteristic of type S—has no prominent bands in the 6800—8800 Å region employed in spectral surveys such as ours. Relative to normal M giants, both S stars and M supergiants show enhanced bands of CN, albeit for different reasons, reflecting a composition difference in one case and a luminosity difference in the other. In addition, stars of both types are likely to show TiO bands that are weak for the star's color; in S stars a deficiency of free oxygen inhibits the formation of TiO, while M supergiants often have colors that are reddened by interstellar dust. Thus a system such as our eight-color photometry which measures TiO, CN, and color cannot distinguish S type giants from reddened M supergiants without additional information. Some S stars—namely, the cooler ones with strong S characteristics—have strong bands of LaO and ZrS in the near infrared which distort the eight-color spectra sufficiently to make these stars recognizable. However, the more typical S stars—the warmer ones with mild S characteristics—cannot be identified by the eight-color photometry and will be misclassified as M supergiants.

Because of this ambiguity, we considered it important to include a ZrO band within the range of our CCD spectra. This was accomplished by extending the spectra shortward to 6400 Å to include the prominent (0,0) band of the γ system which degrades longward from a head at 6474 Å. An alternative solution would be to extend the range longward to include the 9300 Å band of ZrO, but this feature is more difficult to use because of contamination by atmospheric water absorption.

Our CCD spectrum of the S star HD 58881 is shown in Fig. 6. Its most prominent feature by far is the 6474 Å band of ZrO, but it also exhibits very strong CN which depresses the 6800–7400 and 7800–8400 Å regions. From the appearance of the spectrum, it is difficult to be certain whether any TiO is present. The classification S5-/6 quoted in the figure is from Keenan & Boeshaar (1980) and implies that no TiO is present; it should be noted, however, that the star is a small-range variable so that the published type may not be precisely appropriate for the spectrum shown. The eight-color photometry, which measures CN at several places, has consistently confirmed that nearly all the absorption in filter 1 (7120 Å) is due to CN; the greatest amount of TiO that could be present corresponds to a spectral type of K4. Thus the eight-color photometry would classify this star as a moderately reddened K4 Ia supergiant. This classification indicates some useful information about the spectrum of HD 58881, but it is wrong, of course, as regards the reddening, the intrinsic temperature, and the implied distance. Such errors are immediately revealed by checking for the presence of the 6474 Å band of ZrO. Using our CCD spectra, we have found two new S stars which we originally marked as possible M supergiants on the objective-prism plates.

An unexpected result of this survey has been the discovery of a number of heavily reddened supergiants with spectral types in the range early A to late F. These stars appear

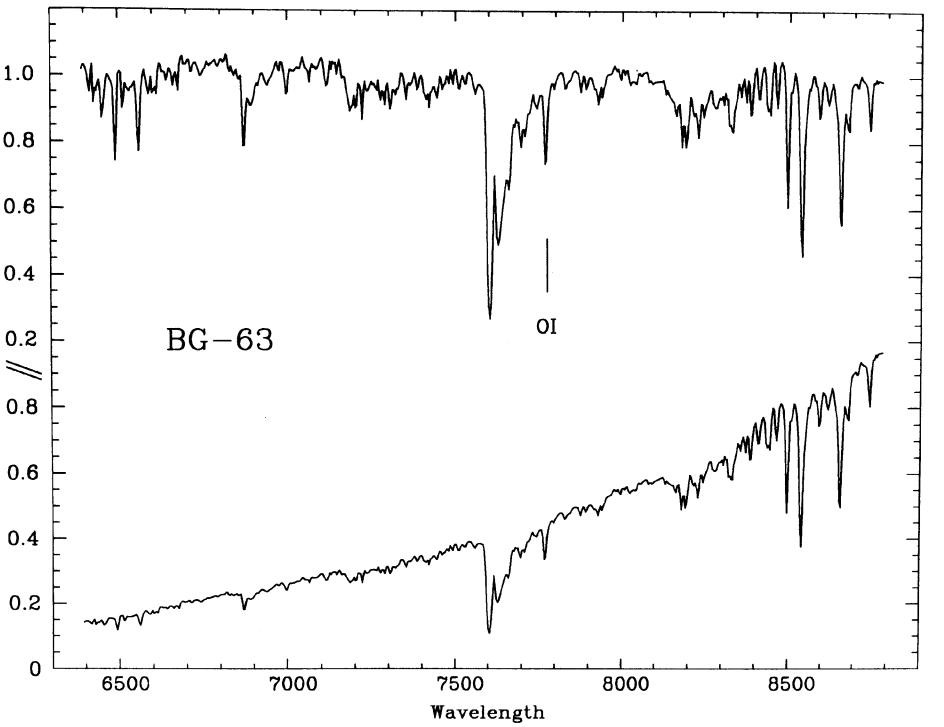

FIG. 7. Flattened and observed spectra of the heavily reddened mid-F supergiant program star BG-63. Note the absence of stellar molecular absorption bands and the presence of the O I feature at 7774 Å, the Ca II triplet, and the Paschen series of hydrogen.

strongly tapered on the objective-prism plates, like reddened early M supergiants. Since these stars have no measurable TiO, the eight-color photometry can say only that they are earlier than K4, and we depend on the CCD spectra for their classification. For these stars we can use the relative strengths of the Ca II lines and the Paschen lines of H as the temperature indicator, while the O I triplet at 7774 Å indicates the luminosity class, being strongest in the brightest supergiants. Figure 7 presents the spectrum of the program star BG-63 ($\alpha = 15{:}27{:}36.2$, $\delta = -57{:}31{:}59$, 1950) which we classify F5 Ia. The figure shows both the flattened spectrum used for classification and the flux-calibrated spectrum, as observed. Our collection of standard-star spectra includes several bright supergiants in the range A–G, and we also use the unpublished atlases of Danks & Dennefeld (1985) and Torres-Dodgen & Weaver (1990).

5. SUMMARY

This is the first paper of a series describing a project designed to locate faint red supergiants belonging to remote arms of the southern Milky Way. Here we have discussed the various techniques used: the survey technique for finding faint red stars likely to be supergiants, the photometric and spectroscopic methods of classifying the candidate stars in two dimensions, and the photometric technique for measuring their interstellar reddening and distances.

Paper II of the series will give results for the longitude interval 210°–240°, a survey area of ~360° sq. involving the constellations Monoceros, Canis Major, and Puppis in which the spectroscopic and photometric follow-up observations are now complete. We have also made substantial headway in the rich Carina region, where supergiants can be found over a great range of distances, and in Norma, where we are attempting to identify distant red supergiants that might help to confirm the existence of an arm interior to the Sagittarius Arm.

All of the observations for this project are made in the near infrared, a region particularly favorable for studying stars that are both intrinsically red and likely to be reddened. By employing low-resolution techniques we have been able to avoid the need for large telescopes. Except for the 2.5 m DuPont telescope at Las Campanas, which we have used to secure spectra of some of the faintest program stars, CTIO telescopes of aperture 1.5 m or smaller have been used for all aspects of this work, mostly during bright time.

Since our search for supergiant candidates on objective-prism plates uses color as the primary (often the only) criterion, we are finding large numbers of supergiants primarily because they tend to be heavily reddened. But in order not to exclude lightly reddened supergiants, we must also mark as candidates a large number of ordinary, moderately reddened giants. We intend to publish our two-dimensional classifications and photometric results for the stars which prove to be giants as well as for the su-

pergiants, since the giants may also be useful in a number of ways. For every classifiable star our data will provide not only a classification but also a measure of its distance and reddening. While the distances of class III giants encountered in this survey place them only within the Local Arm or the nearer interarm regions, they are often noticeably reddened. Thus the giants as well as the supergiants will contribute to our knowledge of the distribution of absorbing matter in the Galaxy.

Our primary objective, of course, is to find distant red supergiants and to learn what we can from them about the spiral-arm structure of the Galaxy (Wing 1989b). The ultimate success of this application hinges on the accuracy of our CN-based distances. Work is currently under way to measure CN indices for red supergiants considered to be members of clusters and associations whose distances can be judged from other data; this we hope will provide both a CN-absolute magnitude relation and an indication of its intrinsic width. Our method appears to be at least as accurate as other photometric methods of distance determination used in the past and should have a decided advantage in heavily obscured regions. Already we have more than doubled the number of M type supergiants known in the Galaxy, and our knowledge of red supergiants in the regions covered by the survey should attain a degree of completeness comparable to that of OB stars so that useful *B/R* ratios can be formed. For these reasons we are confident that the red supergiants found in this study will add a new dimension to our knowledge of the structure of the Galaxy.

We wish to thank the staffs of Cerro Tololo Inter-American Observatory and Las Campanas Observatory for their excellent help in securing the observations for this project; we also thank Nelson Zarate and Steven Hulbert of the Space Telescope Science Institute for their aid in the use of IRAF. E.C. thanks the Departamento Técnico de Investigación of the Universidad de Chile for their support of Proyecto E2602-8712. D.J.M. gratefully acknowledges the support of the American Astronomical Society Small Research Grant Program and of the National Science Foundation through Grant No. 84-21307 to Michigan State University and Computer Sciences Corporation.

REFERENCES

Blaauw, A. 1963, in Basic Astronomical Data, edited by K. Aa. Strand (University of Chicago Press, Chicago), p. 383
Blanco, V. M., & Münch, L. 1955, Bol. Ton. Tac., No. 12, 17
Danks, A. C., & Dennefeld, M. 1985, BAAS, 17, 881
Egret, D., Keenan, P. C., & Heck, A. 1982, A&A, 106, 115
Griffin, R. F., & Redman, R. O. 1960, MNRAS, 120, 287
Hayes, D. S., Latham, D. W., & Hayes, S. H. 1975, ApJ, 197, 587
Hoffleit, D., & Jaschek, C. 1982, The Bright Star Catalogue, 4th ed. (Yale University Observatory, New Haven)
Humphreys, R. M., & Davidson, K. 1979, ApJ, 232, 409
Johnson, H. L. 1968, in Nebulae and Interstellar Matter, edited by B. M. Middlehurst and L. H. Aller (University of Chicago Press, Chicago), p. 167
Jones, J. E., Alloin, D. M., & Jones, B. J. T. 1984, ApJ, 283, 457
Keenan, P. C. 1963, in Basic Astronomical Data, edited by K. Aa. Strand (University of Chicago Press, Chicago), p. 78
Keenan, P. C., & Boeshaar, P. C. 1980, ApJS, 43, 379
Keenan, P. C., & McNeil, R. C. 1989, ApJS, 71, 245
Keenan, P. C., & Yorka, S. B. 1988, Bull. d'Inf. CDS, No. 35, 37
Kurucz, R. L. 1979, ApJS, 40, 1
Lasker, B. M., Sturch, C. R., McLean, B. J., Russell, J. L., Jenkner, H., & Shara, M. M. 1990, AJ, 99, 2019
Lindblad, B. 1922, ApJ, 55, 85
Lockwood, G. W., & Wing, R. F. 1982, MNRAS, 198, 385
MacConnell, D. J. 1988, AJ, 96, 354
MacConnell, D. J. 1989, BAAS, 21, 748
MacConnell, D. J., & Wing, R. F. 1984, BAAS, 16, 970
MacConnell, D. J., Wing, R. F., & Costa, E. 1985, BAAS, 17, 595
MacConnell, D. J., Wing, R. F., & Costa, E. 1986, in Luminous Stars and Associations in Galaxies, IAU Symposium No. 116, edited by C. W. H. de Loore, A. J. Willis, and P. Laskarides (Reidel, Dordrecht), p. 123
MacConnell, D. J., Wing, R. F., & Costa, E. 1987, Rev. Max. Astron. Astrofis., 14, 367
Merrill, P. W. 1934, ApJ, 79, 183
Meylan, G., & Maeder, A. 1983, A&A, 124, 84
Nassau, J. J., Blanco, V. M., & Morgan, W. W. 1954, ApJ, 120, 478
Schild, R. 1967, ApJ, 148, 449
Schild, R., Peterson, D. M., & Oke, J. B. 1971, ApJ, 166, 95
Schulte-Ladbeck, R. E. 1988, A&A, 189, 97
Sharpless, S. 1956, ApJ, 124, 342
Torres-Dodgen, A. V., & Weaver, W. B. 1990, BAAS, 22, 859
Warner, J. W., & Wing, R. F. 1977, ApJ, 218, 105
White, N. M., & Wing, R. F. 1978, ApJ, 222, 209
Wildey, R. L. 1964, ApJS, 8, 439
Wing, R. F. 1967a, in Colloquium on Late-Type Stars, edited by M. Hack (Osservatorio Astronomico di Trieste), p. 205
Wing, R. F. 1967b, Ph.D. dissertation, University of California, Berkeley
Wing, R. F. 1971, in Proceedings of the Conference on Late-Type Stars, edited by G. W. Lockwood and H. M. Dyck, KPNO Contr. No. 554, p. 145
Wing, R. F. 1973, in Spectral Classification and Multicolour Photometry, IAU Symposium No. 50, edited by Ch. Fehrenbach and B. E. Westerlund (Reidel, Dordrecht), p. 209
Wing, R. F. 1979, in Problems of Calibration of Multicolor Photometric Systems, edited by A. G. D. Philip (Dudley Observatory Report No. 14), p. 499
Wing, R. F. 1989a, in The Gravitational Force Perpendicular to the Galactic Plane, edited by A. G. D. Philip and P. K. Lu (Davis, Schenectady), p. 167
Wing, R. F. 1989b, Rev. Max. Astron. Astrofis., 19, 57
Wing, R. F., Gustafsson, B., & Eriksson, K. 1985, in Calibration of Fundamental Stellar Quantities, IAU Symposium No. 111, edited by D. S. Hayes, L. E. Pasinetti, and A. G. D. Philip (Reidel, Dordrecht), p. 571
Wing, R. F., & Lockwood, G. W. 1973, ApJ, 184, 873
Wing, R. F., MacConnell, D. J., & Costa, E. 1987, Rev. Max. Astron. Astrofis., 14, 362
Wing, R. F., & White, N. M. 1978, in The *HR* Diagram, IAU Symposium No. 80, edited by A. G. D. Philip and D. S. Hayes (Reidel, Dordrecht), p. 451
Wing, R. F., & Yorka, S. B. 1979, in Spectral Classification of the Future, IAU Colloquium No. 47, edited by M. F. McCarthy, A. G. D. Philip, and G. V. Coyne (Vatican Observatory), p. 519.